

LETTERS

Energy input and response from prompt and early optical afterglow emission in γ -ray bursts

W. T. Vestrand¹, J. A. Wren¹, P. R. Wozniak¹, R. Aptekar², S. Golentskii², V. Pal'shin², T. Sakamoto³, R. R. White¹, S. Evans¹, D. Casperson¹ & E. Fenimore¹

The taxonomy of optical emission detected during the critical first few minutes after the onset of a γ -ray burst (GRB) defines two broad classes: prompt optical emission correlated with prompt γ -ray emission¹, and early optical afterglow emission uncorrelated with the γ -ray emission². The standard theoretical interpretation attributes prompt emission to internal shocks in the ultra-relativistic outflow generated by the internal engine^{3–5}; early afterglow emission is attributed to shocks generated by interaction with the surrounding medium^{6–8}. Here we report on observations of a bright GRB that, for the first time, clearly show the temporal relationship and relative strength of the two optical components. The observations indicate that early afterglow emission can be understood as reverberation of the energy input measured by prompt emission. Measurements of the early afterglow reverberations therefore probe the structure of the environment around the burst, whereas the subsequent response to late-time impulsive energy releases reveals how earlier flaring episodes have altered the jet and environment parameters. Many GRBs are generated by the death of massive stars that were born and died before the Universe was ten per cent of its current age^{9,10}, so GRB afterglow reverberations provide clues about the environments around some of the first stars.

On 20 August 2005 a relatively faint 30-s pulse of γ -ray emission from GRB 050820a started at 06:34:53 Universal Time (UT), and was localized¹¹ in real time by the autonomous software of the Burst Alert Telescope (BAT) on the Swift satellite¹². One of our autonomous RAPTOR (Rapid Telescopes for Optical Response) telescopes¹³ began optical imaging of the GRB 050820a location 5.5 s (ref. 14) after distribution of the Swift alert. The images show emergence of faint optical emission that suddenly flares (see Fig. 1) and varies erratically before gradually fading over the course of the first hour. Comparison of the optical measurements with the γ -ray light curve measured by the KONUS-Wind experiment (Fig. 2) indicates that the rapid optical flares are simultaneous with the major outbursts of γ -ray emission. These data clearly confirm the idea that one component of the early optical light from GRBs is prompt emission that closely tracks the γ -ray emission¹. The remaining optical emission persists even after the γ -rays disappear and can naturally be explained as an early afterglow component^{2,15–18}.

The optical light curve rise to maximum light for even the afterglow component has too much curvature (positive and negative) to be fitted by the self-similar power-law rise predicted by internal or external shock models. To dissect the light curve into primary components, we made the simple conjecture that the two optical components—prompt optical $F_p(t)$ and early optical afterglow $F_a(t)$ fluxes—have the temporal behaviours:

$$F_p(t) = C_p F_\gamma(t) \quad (1)$$

$$F_a(t) = C_a \left(\frac{t - t_o}{t_o} \right)^{-s} \exp \left(\frac{-\tau}{t - t_o} \right) \quad (2)$$

Here $F_\gamma(t)$ is the prompt γ -ray flux; t_o is the time for onset of energy release; τ is the timescale for rise of the afterglow; s is the power-law

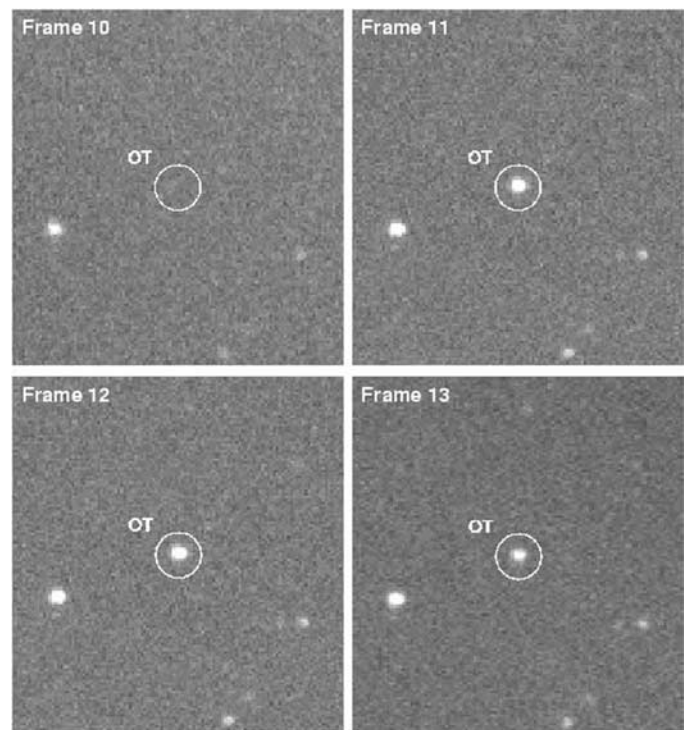


Figure 1 | The onset of prompt optical emission from GRB 050820a. The images show the GRB location in four consecutive frames collected by the 0.4-m fully autonomous rapid-response telescope, RAPTOR-S, owned by the Los Alamos National Laboratory and located at an altitude of 2,500 m in the Jemez Mountains of New Mexico. The RAPTOR-S telescope uses an unfiltered 1,000 × 1,000 pixel back-illuminated charge-coupled device (CCD) camera and typically achieves a 5-sigma limiting magnitude of $R \approx 19$ mag for 30-s exposures. The displayed images span the time interval 06:38:07.2 to 06:40:50.7 UT on 20 August 2005 and the circle denotes the location of the GRB optical counterpart (right ascension 22 h 29 min 38.1 s, declination $+19^\circ 33' 37.1''$ (J2000))²⁶ that subsequent spectral measurements^{27,28} showed was at a redshift of $z = 2.612 \pm 0.002$. The top two images (frames 10 and 11) show flaring of the optical transient (OT) by more than two magnitudes in less than 30 s. The bottom two images (frames 12 and 13) are the next two 30-s exposures that show an abrupt drop of the optical emission in frame 13 by ~ 0.5 magnitudes.

¹Los Alamos National Laboratory, Space Science and Applications Group, ISR-1, MS-D466, Los Alamos, New Mexico 87545, USA. ²Ioffe Physico-Technical Institute, St Petersburg, 194021, Russia. ³NASA Goddard Space Flight Center, Code 661, Greenbelt, Maryland 20771, USA.

decay index; and C_p, C_a are the relative amplitudes of the prompt and early afterglow components, respectively. After re-binning the γ -ray measurements to the same observing intervals as the optical observations (see Table 1), we find that the simple temporal behaviours given by equations (1) and (2) jointly describe the optical light curve measured for GRB 050820a rather well (see Fig. 3).

The prompt optical component given by equation (1) reproduces the fast variations observed in the RAPTOR light curve when the KONUS γ -ray measurements are scaled by the flux ratio $C_p = F_{opt}/F_\gamma \approx 7 \times 10^{-6}$ —a ratio is comparable to the value of $F_{opt}/F_\gamma = 1.2 \times 10^{-5}$ found for GRB 041219a¹. For both events there

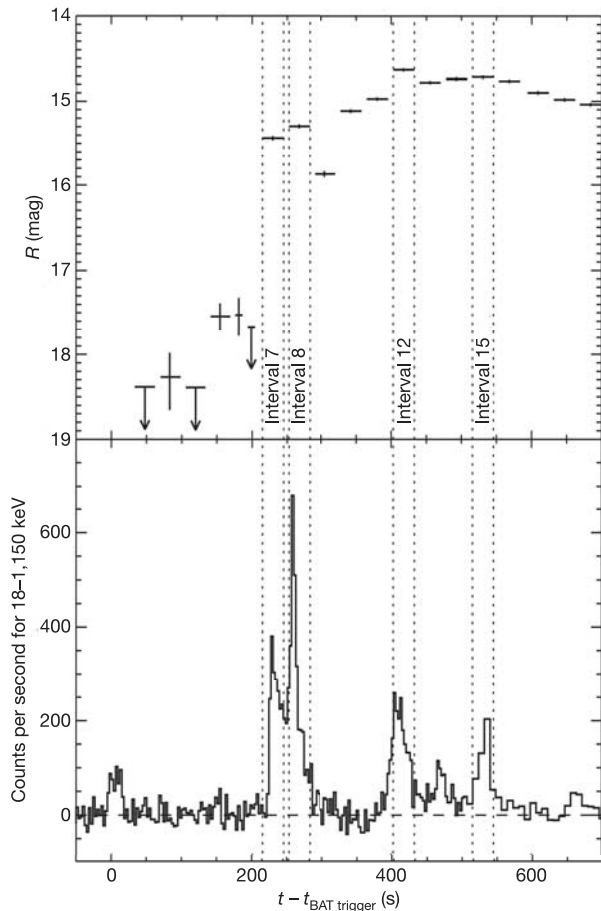


Figure 2 | A comparison of the early optical light curve and the γ -ray light curve measured for GRB 050820a. The lower panel shows the γ -ray count rate in the light curve measured by KONUS γ -ray detectors on board the WIND satellite. The upper panel shows the optical light curve measured by the RAPTOR-S telescope. The horizontal lines in the upper panel denote the durations of the observation intervals and the vertical lines denote the 1-sigma error bars associated with the optical magnitude measurements made during those intervals. After that initial pulse, the GRB was quiescent at γ -ray energies for more than three minutes until a major outburst began at 06:38:40 UT. The observations by Swift were truncated by satellite passage into a high background region, but the KONUS γ -ray detector aboard the Wind satellite was able to measure the entire complex γ -ray light curve²⁹, which lasted ~ 750 s. Integrated over the entire event, the total (18–1,000 keV) γ -ray fluence for GRB 050820a was 5.3×10^{-5} erg cm⁻², which for the observed redshift^{27,28} ($z = 2.6$) and standard cosmological parameters ($\Omega_m = 0.3, \Omega_\Lambda = 0.7, H_0 = 70$ km s⁻¹ Mpc⁻¹) corresponds to an isotropic energy of 8.1×10^{53} erg. The abrupt brightening of the optical emission shown in Fig. 1 occurs simultaneously with the major pulses of γ -ray emission shown in the interval between 226 and 290 s after the burst trigger. The onset of early optical afterglow emission is visible in the interval between 300 and 400 s after the burst trigger. $t_{BAT\ trigger}$ time that BAT was triggered.

Table 1 | Joint RAPTOR/KONUS observations of GRB 050820a

Interval	t_{start} (s)	t_{end} (s)	Δt_{exp} (s)	R (mag)	$F(18-1,000\text{ keV})$ (10^{-7} erg cm ⁻²)
0	-4.30	19.30	23.6	—	25.9 ± 1.3
1	33.72	61.87	30	>18.38	<3.3
2	70.08	98.27	30	18.270 ± 0.290	<4.5
3	105.97	133.56	30	>18.39	<6.0
4	141.16	168.76	20	17.540 ± 0.150	<5.6
5	176.35	186.35	10	17.530 ± 0.200	<2.2
6	194.05	204.05	10	>17.67	<3.7
7	214.85	244.85	30	15.437 ± 0.025	101.9 ± 1.4
8	252.44	282.44	30	15.297 ± 0.024	160.2 ± 1.5
9	290.04	320.04	30	15.870 ± 0.033	16.6 ± 1.2
10	327.63	357.63	30	15.115 ± 0.022	<5.1
11	365.23	395.23	30	14.972 ± 0.020	7.8 ± 1.1
12	420.83	432.83	30	14.633 ± 0.019	87.7 ± 1.2
13	440.42	470.42	30	14.779 ± 0.019	27.7 ± 1.2
14	478.11	508.11	30	14.740 ± 0.020	21.5 ± 1.1
15	515.71	545.71	30	14.718 ± 0.019	51.5 ± 1.1
16	553.30	583.30	30	14.764 ± 0.019	11.5 ± 1.1
17	594.20	624.20	30	14.901 ± 0.020	4.7 ± 3.3
18	631.79	661.79	30	14.983 ± 0.020	<5.4
19	669.39	699.39	30	15.038 ± 0.021	11.9 ± 1.1
20	706.98	736.98	30	15.060 ± 0.022	11.5 ± 1.3

The R-band magnitudes were derived by transforming the unfiltered measurements to an R-band equivalent using the USNO-B1.0 magnitudes for comparison stars in the RAPTOR images.

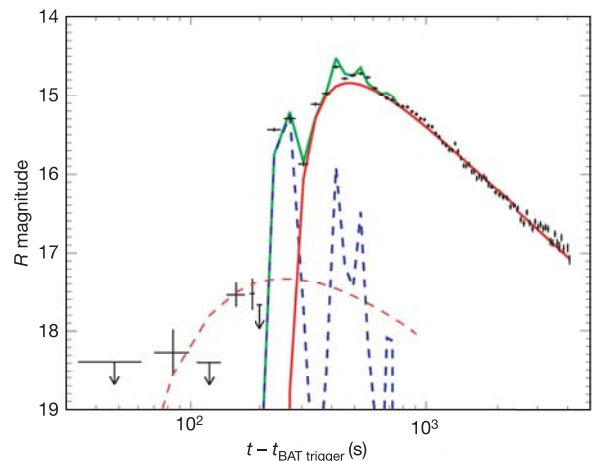


Figure 3 | The decomposition of the optical light curve measured for GRB 050820a into primary optical components. The R-band magnitudes measured by RAPTOR-S are indicated by the black crosses, with observing intervals denoted by horizontal lines and 1-sigma error bars represented by the vertical lines. The blue dashed trace shows the prompt optical component obtained by scaling the KONUS γ -ray flux measurements, after re-binning to the same time intervals as the RAPTOR measurements, by the factor $F_{opt}/F_\gamma = 7.4 \times 10^{-6}$ and converting to the R-band equivalent magnitude. The solid red line shows the model early afterglow component of the form given by equation (2) with a flux-rise timescale of $\tau \approx 280$ s, the late-time power-law flux decay with index $s \approx 1.1$, and a reference time t_o equal to the start of the dominant γ -ray outburst (226 s after the BAT trigger time). The green trace shows the sum of these prompt and early afterglow model components. The dashed red line shows an afterglow with the same flux-rise timescale as the dominant afterglow component ($\tau \approx 280$ s) but with a reference time appropriate for the precursor pulse ($t_o = 5$ s) and an amplitude given by the ratio of the γ -ray fluence for the precursor pulse to that of the main (18–1,150 keV) pulse of 0.1. We note that even when the prompt γ -ray-emitting intervals are dropped, the rise of the afterglow emission cannot be fitted with a power-law dependence. By fitting a power law with a reference time of $t_o = 0.0$ to the fast rise in the interval, measured with unprecedented signal-to-noise between 300 and 400 s after the trigger, we predict fluxes that are inconsistent with the detections of optical emission by RAPTOR and the UVOT in the interval before 200 s after the trigger.

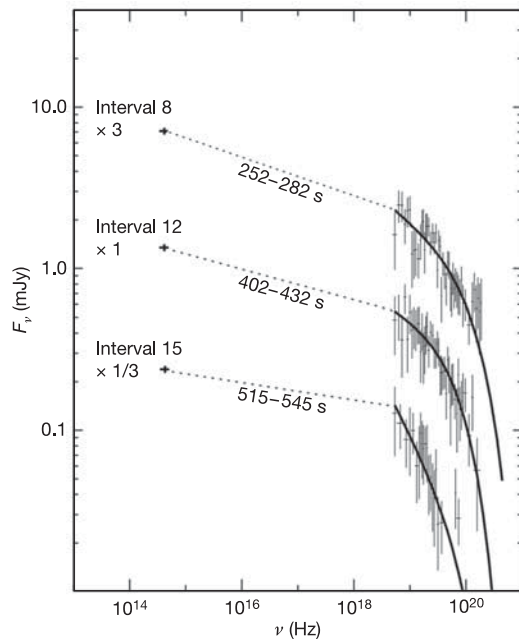


Figure 4 | Broadband spectra of prompt emission from GRB 050820a. These spectra are constructed from simultaneous optical measurements from the RAPTOR-S telescope and γ -ray measurements from the KONUS experiment on board the WIND satellite. The crosses at the low frequencies denote the optical flux density after correction for the contribution from early optical afterglow emission. The solid line denotes the best-fitting model for the KONUS measurements and the high-frequency crosses represent the individual channel measurements with the 1-sigma errors. The time intervals are measured in seconds from the Swift trigger time. During intervals 8 and 12, the broadband spectra of prompt emission for GRB 050820a show optical flux density levels that are roughly consistent with an extrapolation of the high-energy spectral shape. But in interval 15, extrapolation of the γ -ray spectrum underpredicts the optical flux. This suggests that the prompt optical and γ -ray emission might be generated by separate, but closely linked, radiation processes.

are intervals in which the broadband prompt spectra (Fig. 4) between optical and γ -ray bands must on average be flatter than the $F_\nu \propto \nu^{-1/2}$ expected for the standard synchrotron picture with fast cooling electrons and a cooling critical frequency near the optical band⁷. A possible explanation for closely linked, but separate, spectral components is that they are both associated with the internal jet shock, but that optical emission is generated by the reverse shock and γ -rays by the forward shock⁷. This scenario would place bounds on the jet bulk velocity, the overtaking shell thickness, and the distance at which the emission originates. An alternate internal shock explanation is that the optical light is synchrotron emission and the γ -rays are inverse-Compton-scattered synchrotron photons⁴. The closer tracking of the optical flux with the highest-energy γ -ray band also seen in GRB 041219a is naturally explained in this scenario. Detailed modelling work will be needed to test the standard synchrotron picture and, if necessary, discriminate between possible alternative models, but the close temporal tracking of the prompt components will place important constraints on the jet properties, which are difficult to obtain in other ways.

The dramatic optical flux increase immediately after the dominant γ -ray pulse suggests that the afterglow is associated with the impulsive energy release signalled by the prompt emission. After the rapid initial rise, the rate of flux increase slows and transitions into a shallow decline that gradually steepens to a power-law flux decay with an index of $s = 1.1$ after $\sim 10^3$ seconds. Similar late-time behaviour has been observed for several other events^{18,19} and is consistent with that expected for an external forward shock in the internal/external shock paradigm.

Although neither instrument was observing the GRB location during the precursor pulse that triggered Swift/BAT, both RAPTOR and the Ultra-Violet and Optical Telescope (UVOT) on Swift did detect²⁰ faint optical emission during the interval after the precursor and before the outburst of intense γ -ray emission. During that same interval neither Swift nor KONUS detected γ -ray emission. The best explanation for this faint optical emission is that it is afterglow emission from the precursor γ -ray pulse—an explanation supported by the Swift detection of a fading soft X-ray afterglow during the same interval²¹. Further, the RAPTOR measurements of this precursor afterglow show a light curve shape that is consistent with a straightforward scaling of the main afterglow (Fig. 3).

Until now, observational determination of the light curve shape has been hampered by not knowing where to place the onset reference time t_0 (refs 22, 23). In other words, when does the afterglow begin? Often it is placed at the burst trigger time, but it can be placed logically anywhere within, or even before, the γ -ray-emitting interval. The exact choice can substantially modify the derived shape of the early light curve^{22,23}. Our observations show: (1) that the onset of the dominant afterglow component should be referenced to the time of the onset of the dominant γ -ray pulse; and (2) that the assumption of a single onset time for the afterglow, t_0 , is too simple. The structure of the afterglow is better understood as a reverberation that can be related to the stimulus measured by the prompt emission convolved with a transfer function representing the response of the system.

There is growing evidence that the GRB engine can impulsively release energy well after the initial explosion^{24,25}. Measurements of the broad-band spectra of the prompt emission place important constraints on the evolution of the jet itself. Structure associated with the afterglow from those secondary energy releases can also emerge as the primary afterglow component fades. The timing and strength of those secondary reverberations will probe the evolution of the interaction and how the GRB environment is modified. Long-duration GRBs are known to signal the deaths of massive stars and occur at very high redshift^{9,10}, so measurement of GRB reverberation and its temporal variations can be used to map out the nurseries of the earliest stars.

Received 1 February; accepted 15 May 2006.

- Vestrand, W. T. *et al.* A link between prompt optical and prompt γ -ray emission in γ -ray bursts. *Nature* **435**, 178–180 (2005).
- Akerlof, C. *et al.* Observations of contemporaneous optical radiation from a γ -ray burst. *Nature* **398**, 400–402 (1999).
- Fenimore, E. E., Madras, C. D. & Nayakshin, S. Expanding relativistic shells and gamma-ray burst temporal structure. *Astrophys. J.* **473**, 998–1012 (1996).
- Meszáros, P. & Rees, M. GRB 990123: reverse and internal shock flashes and late afterglow behaviour. *Mon. Not. R. Astron. Soc.* **306**, L39–L43 (1999).
- Katz, J. Low-frequency spectra of gamma-ray bursts. *Astrophys. J.* **432**, L107–L109 (1994).
- Meszáros, P. & Rees, M. Optical and long-wavelength afterglow from gamma-ray bursts. *Astrophys. J.* **476**, 232–237 (1997).
- Sari, R. & Piran, T. Predictions for the very early afterglow and the optical flash. *Astrophys. J.* **520**, 641–649 (1999).
- Panaiteanu, A. & Kumar, P. Analysis of two scenarios for the early optical emission of the gamma-ray burst afterglow 990123 and 021211. *Mon. Not. R. Astron. Soc.* **353**, 511–522 (2004).
- Lamb, D. Q. & Reichart, D. E. Gamma-ray bursts as a probe of the very high redshift universe. *Astrophys. J.* **536**, 1–18 (2000).
- Ciardi, B. & Loeb, A. Expected number and flux distribution of gamma-ray burst afterglows with high redshifts. *Astrophys. J.* **540**, 687–696 (2005).
- Page, M. *et al.* GRB 050820: Swift detection of a GRB. *GRB Circ. Netw.* **3830** (2005).
- Gehrels, N. *et al.* The Swift gamma-ray burst mission. *Astrophys. J.* **611**, 1005–1020 (2004).
- Vestrand, W. T. *et al.* The RAPTOR experiment: a system for monitoring the optical sky in real time. *Proc. SPIE* **4845**, 126–136 (2002).
- Wren, J. *et al.* GRB050820: Early RAPTOR detections. *GRB Circ. Netw.* **3836** (2005).
- Van Paradijs, J., Kouveliotou, C. & Wijers, R. A. M. J. Gamma ray burst afterglows. *Annu. Rev. Astron. Astrophys.* **38**, 379–425 (2000).
- Li, W. *et al.* The early light curve of the optical afterglow of GRB 021211. *Astrophys. J.* **586**, L9–L12 (2003).

17. Fox, D. W. *et al.* Early optical emission from the γ -ray burst of 4 October 2002. *Nature* **422**, 284–286 (2003).
18. Wozniak, P. R. *et al.* RAPTOR observations of the early optical afterglow from GRB 050319. *Astrophys. J.* **627**, L13–L16 (2005).
19. Rykoff, E. S. *et al.* The early optical afterglow of GRB 030418 and progenitor mass loss. *Astrophys. J.* **601**, 1013–1018 (2004).
20. Chester, M. *et al.* Swift/UVOT photometry of GRB 050820. *GRB Circ. Netw.* **3838** (2005).
21. Page, K. L. *et al.* GRB 050820: refined XRT analysis. *GRB Circ. Netw.* **3837** (2005).
22. Lazzati, D. & Begelman, M. Thick fireballs and the steep decay in the early X-ray afterglow of gamma-ray bursts. *Astrophys. J.* **641**, 972–977 (2006).
23. Quimby, R. M. *et al.* Early-time observations of the GRB 050319 optical transient. *Astrophys. J.* **640**, 402–406 (2006).
24. Falcone, A. D. *et al.* The giant x-ray flare of GRB 050502b: evidence for late-time internal engine activity. *Astrophys. J.* **641**, 1010–1017 (2006).
25. Wozniak, P. R. *et al.* RAPTOR observations of delayed explosive activity in the high-redshift gamma-ray burst GRB 060206. *Astrophys. J.* **642**, L99–L102 (2006).
26. Fox, D. B. & Cenko, S. B. GRB 050820: Optical afterglow from P60. *GRB Circ. Netw.* **3829** (2005).
27. Prochaska, J. X. *et al.* GRB 050820: High resolution spectroscopy from Keck. *GRB Circ. Netw.* **3833** (2005).
28. Ledoux, C. *et al.* VLT/UVES spectroscopy of GRB050820. *GRB Circ. Netw.* **3869** (2005).
29. Golenetskii, S. *et al.* GRB050820a—a very long GRB like GRB041219a? Konus-Wind Observation. *GRB Circ. Netw.* **3852** (2005).

Acknowledgements The RAPTOR project is supported by the Laboratory Directed Research and Development program at Los Alamos National Laboratory. The Konus-Wind experiment is supported by the Russian Space Agency and the Russian Foundation for Basic Research.

Author Information Reprints and permissions information is available at npg.nature.com/reprintsandpermissions. The authors declare no competing financial interests. Correspondence and requests for materials should be addressed to W.T.V. (vestrand@lanl.gov).